Maritime Engineering
Volume 165 Issue MA2
Tsunami and wind-driven wave forces in the Mediterranean Sea
Camilleri

ice | proceedings

Proceedings of the Institution of Civil Engineers
Maritime Engineering 165 June 2012 Issue MA2
Pages 65–79 http://dx.doi.org/10.1680/maen.201024
Paper 201024
Received 20/07/2010 Accepted 06/07/2011
Keywords: disaster engineering/maritime engineering/sea defences

Institution of Civil Engineers
publishing

Tsunami and wind-driven wave forces in the Mediterranean Sea

Denis H. Camilleri Eur Ing, BSc(Eng), BA(Arch), CEng, ACIArb, FIStructE, FICE
Managing partner, dhi Periti, Europa Centre, Floriana, Malta

The comparison between the impact forces generated from a tsunami wave and those from a wind-driven wave are presented here. Wind-driven wave forces are derived from established maritime theory going back to the nineteenth century. The understanding of tsunami impact forces is derived from more recent research correlated further by some recent model testing. The maritime theory on wave impact force for breaking and non-breaking waves is very well developed from breakwater/seawall engineering. It commenced with Stephenson and Hiro's nineteenth century rule of thumb equations, which was then followed in the twentieth century by Sainflou's theory (1928) for standing waves in deep water. Minikin's studies in the 1950s yielded results for breaking waves and noted high dynamic localised loads and these was followed in 1985 by Goda's equations applicable for both breaking and non-breaking waves. At Alderney, typical impact pressures of 40 t/m^2 (400 kN/m^2) for 20 m/s waves were recorded, although a Ciria document published in 1992 notes that the average wave pressure on sea walls varies from 150 kN/m^2 down to 50 kN/m^2 pressure. Users are cautioned about the extremely high wave forces associated with the Minikin method. In 1984, Blackmore and Hewson developed a method to estimate an average wave pressure from broken wave loads. The present analysis which was undertaken for the bathymetry and climatological data of the Mediterranean Sea then outlines the Malta scenario. It can act as a guide to structural engineers in selecting suitable values for the impact pressures that vertical walls may be subjected to for the cases of wind-driven or tsunami waves.

Notation

A	wave amplitude
B	frontal wall area
C_d	drag coefficient
C_m	inertia coefficient
D	water depth (m)
dU/dt	total water particle acceleration
E	energy per unit length of regular sinusoidal wave crest/wavelength
F	fetch length in km or nautical miles (1 nautical mile = 1858 m)
F_D	drag force
F_h	horizontal force
F_{min}	minimum fetch length (nautical miles)
F_t	total tsunami force
F_w	hydrostatic force
F_I	inertia force
g	gravitation of the Earth (9·81 m/s^2)
H	still water depth for a shallow wave location where wave height is much smaller than water depth
H_{max}	maximum height of wave (m)
H_s	significant height (m)
I	tsunami intensity
L	wavelength from crest to crest of the wave (m)
P	uniform pressure of the vertical wall
T	wave period
t	time (ms)
t_{min}	minimum duration (h)
T_s	significant period (s)
U	water particle velocity
U_k	wind speed in knots (1 knot = 0·516 m/s)
v_c	velocity of the breaker at the wall = $(gd)^{1/2}$
λ	aeration coefficient taken as 0·3 for a sand bed and 0·6 for a rock bed
ρ_w	density of seawater given as 1025 kg/m^3

1. Introduction

The force of some tsunamis is enormous. Boulders with masses around 200 t (5 m across) can be displaced inland by hundreds of metres by tsunami surges only 10 m deep, whereas theoretical short period storm waves with heights of 100–150 m are required to produce the same movement. The very largest wave-displaced boulders recorded, found in the

Bahamas on ridges 40 m above mean sea level, with a mass of 2000 t imply tsunami surges of 30 to 40 m depth.

On the other hand, it is very improbable for wind-driven waves as an example to be higher than 12 m, with boulders up to 15 t in weight being washed over sea walls 4 m above sea level.

The horizontal forces acting on a structure under a tsunami given by Okada *et al.* (2004) is a form of the Morrison equation. In maritime engineering, this is used to calculate drag and inertia forces due to non-breaking waves for circular pile structures. Interest in tsunami force all started in the early 1990s. The Building Centre of Japan recommends using a wave height against a building of three times the maximum approach depth. Recent model testing has indicated the maximum wave loading on house walls for the same force at wave impact is about 10 to 12 times the hydrostatic force.

2. The physics of waves and bathymetry data

The characteristics of the different types of sea waves are given in Table 1.

The extraordinary long wavelength produced during tsunamis, as given in kilometres in Table 1, classifies a tsunami wave as a shallow water wave.

2.1 Shallow waves

Shallow waves are defined for $D/L < 1/20$ and the velocity V is given by

$$V = (gD)^{0{\cdot}5} = 3{\cdot}1(D)^{0{\cdot}5} \quad (1)$$

where g is the gravitation of the Earth (9·81 m/s^2); D is the water depth (m); and L is the wavelength (m) from crest to crest of the wave.

Thus noting that the deepest ocean seas which stand at 10 000 m, whereas the deepest end of the Mediterranean is 4000 m, the sea depth to wavelength ratio for a tsunami wave stands at 200 km/4 km = 50 > 20, and thus is defined as a shallow wave.

2.2 Deep water waves

Deep water waves are defined for $D/L > 1/2$

$$V = (gL/2\pi)^{0{\cdot}5} = 1{\cdot}25L^{0{\cdot}5} \quad (2)$$

From conservation of energy, wave height varies with depth and is given by

$$H_2 = H_1(y_1/y_2)^{1/4} \quad (3)$$

where H is the depth (m) of the wave from crest to trough; and y_1 and y_2 are defined as the water depth at particular locations.

Wave break is approximately given by $D = 1{\cdot}28H$ or $L = 7H$, with H/L being known as the steepness ratio. Another limiting criterion is the crest angle, which must not be not less than 120°.

Wave height H is an important wave characteristic, but its effect on a structure largely depends on the wave period.

The bathymetry data for the Mediterranean Sea indicate that the maximum depths encountered in the Ionian Sea exceed 4000 m; however, in the Tyrrhenian and Ligurian Sea (Figure 1), the depth rarely exceeds 2000 m. In the Malta Plateau, which extends between Malta and Sicily, the depth rarely exceeds 200 m. The same may be said of the extensive Tunisian Plateau which reaches Lampedusa; here again the depth is limited to less than 200 m, as also in the Gulf of Venice at the top part of the Adriatic Sea. On the other hand the depth in the area between Malta and Libya just exceeds 1000 m at the Malta end. In the eastern Mediterranean from Cyprus up to Israel/Lebanon the sea depth is again limited to within 2000 m.

Wave type	Typical wavelength	Disturbing force
Wind wave	60–150 m	Wind over ocean
Seiche	Large, variable, a function of basin size	Change in atmospheric pressure, storm surge, tsunami
Seismic sea wave (tsunami)	200 km	Faulting of sea floor, volcanic eruption, landslide
Tide	½ circumference of earth – diurnal	Gravitational attraction, rotation of earth

Data source: Garrison (2002)

Table 1. The disturbing forces and typical wavelengths for wind-driven waves, seiches, tsunami and tides

Figure 1. Mediterranean basin and its seas, averaging 3700 km × 1785 km; source: Google Earth, with indication of shallow and deep seas in the Mediterranean. Image © 2011 DigitalGlobe, data SIO, NOAA, US Navy, GEBCO; image © 2011 GeoContent; © 2011 Cnes/Spot Image

Various wind fetches from the Maltese islands are also indicated for various directions.

Normally all continents and lands bordering the sea are surrounded by a 1° (1:55) 1ow gently sloping submerged plain, being an underwater extension of the coastal plain, called the continental shelf. The shallow 130 m deep water normally extends for 78 km leading on to the continental shelf break, marked by an increase in slope. The abysmal zone below 1800 m extends downwards to great depths.

The run-up height R from the conservation of energy flux equation is given by (Chesley and Ward, 2006)

4. $$R = A^{4/5} h^{1/5}$$

where A is the wave amplitude and h is the still water depth for a shallow wave location where wave height is much smaller than water depth.

A train of waves travelling through still water appears to move at half the speed of the individual waves, with the energy being one-half potential and one-half kinetic.

The energy, E, per unit length of regular sinusoidal wave crest/wavelength from linear wave theory, assuming no loss of energy, is given by

5. $$E = \rho_w g L H^2 / 8$$

where ρ_w is the density of the sea given as 1025 kg/m^3, with the other notation as defined previously.

The potential energy density is equal to the kinetic energy, both contributing half to the wave energy density; while doubling the wave height quadruples the wave energy.

The total horizontal force is given by the addition of the hydrostatic, hydrodynamic impulsive and inertial forces acting on the impinging structure. The vertical force is given by the buoyancy forces, hydrodynamic lift and weight of water inside the structure

3. Wind-driven waves

Waves grow continuously under the action of wind and their maximum height reflects the average intensity of the wind along the fetch. Once fully developed, wind waves will not develop in size, no matter how long the wind blows – they are in equilibrium. There is a big difference between the Atlantic and Mediterranean wave heights due to their fetch.

The Maestrale (Figure 2) is the dominant north-westerly wind blowing over most of the western Mediterranean Sea. High waves are present over most of the Mediterranean Sea, tending to reach maximum value where strong wind and long fetch are present simultaneously.

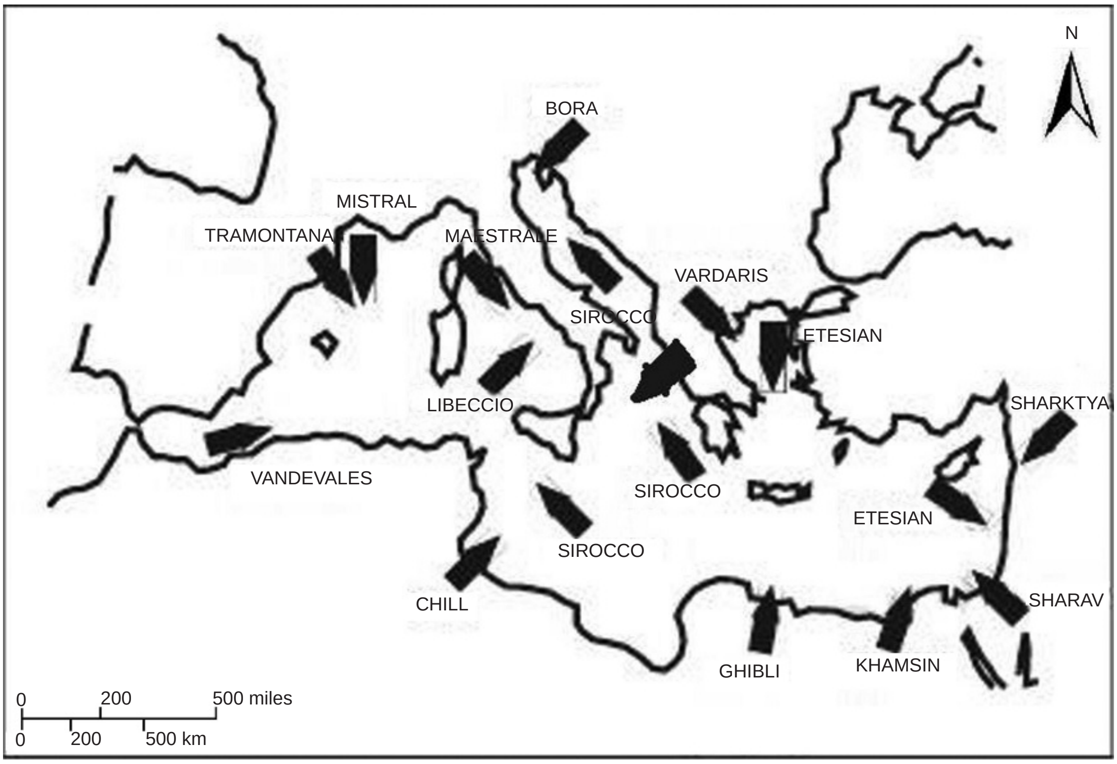

Figure 2. Location and direction of main winds in the Mediterranean region, not to scale. Source: Lionello *et al*. (2006)

The largest maximum waves of 6 m or more are located in the western Mediterranean and the Ionian Sea under the action of the Maestrale. The island of Crete interrupts the fetch of the Etasian winds (Figure 2) and determines two maxima, one in the Aegean and another in the Levantine Basin (Figure 1). The Sirocco (Figure 2) produces the maximum south-westerly winds in the Northern Ionian and the Southern Adriatic (Figure 1).

A 40-year analysis of significant wave heights (Figure 3) shows wave heights in the Mediterranean Basin varying from a minimal effect up to 5 m tending to 7 m, despite the relatively low fetches in comparison with oceanic conditions, although extraordinary storms with wave heights of 10 to 11 m have been recorded. Note that the Malta significant wave height is indicated as 3 m in Figure 3.

Table 2 indicates that for a wave height of 4 m to be developed, a fetch of 518 km on a continued wind speed of 56 km/h is required for a 23 h duration, having an average wavelength of 75 m for a wave period of 8·6 s. These conditions, which relate to the Southern Ocean with winds blowing continuously along the direction of effective fetch, are possibly not applicable to the Mediterranean Sea, being solely of a theoretical application.

The well-known harbour engineer Thomas Stephenson developed the empirical formula, linking fetch and maximum height of wave

6. $$H_{\max} = 0{\cdot}336(F)^{0{\cdot}5}$$

where $H_{\max}$ is the maximum height of wave in metres and F is the fetch or distance in kilometres.

The results of observations to compare data with this formula, based on storms off the Scottish Coast with limited fetch, have been found to be good for fetches up to 1500 km (Minikin, 1963).

At the 1957 Coastal Engineering Conference, Bretschneider (1957) introduced an improved version of the Sverdrup–Munk method. By considering short fetches and high wind speeds, the following formulae giving useful first approximations were derived

7. $$H_{\mathrm{s}} = 0{\cdot}0169\left(U_{\mathrm{k}}^2 F\right)^{0{\cdot}5}$$

8. $$T_{\mathrm{s}} = 0{\cdot}50\left(U_{\mathrm{k}}^2 F\right)^{0{\cdot}25}$$

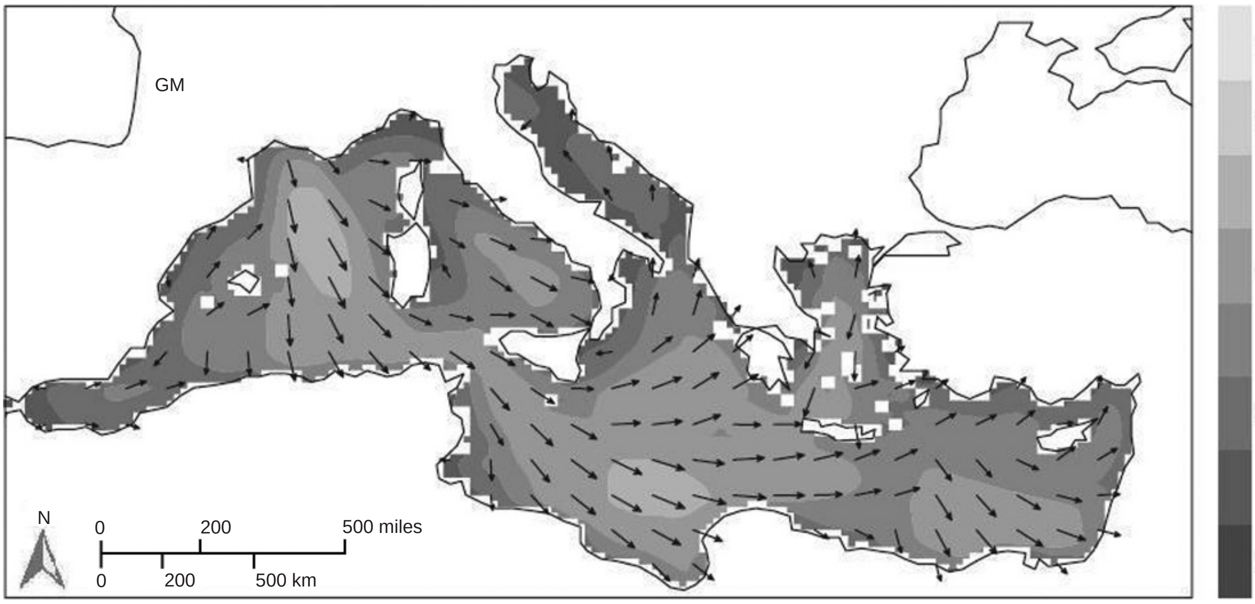

Figure 3. Distribution of maximum wave height, with heights in the key given in metres. Source: Lionello and Sanna (2005)

9. $$F_{\min}/t_{\min} = 0{\cdot}57\left(U_k^2 F\right)^{0{\cdot}25} = 1{\cdot}14 T_s$$

where H_s is the significant height (m); T_s is the significant period (s); U_k is the wind speed in knots (1 knot = 0·516 m/s); F is the fetch length in nautical miles (1 nautical mile = 1858 m); $F_{\min}$ is the minimum fetch length (nautical miles); and $t_{\min}$ is the minimum duration (h).

The value of F to be used in Equation 7 must be equal to or less than $F_{\min}$ obtained from Equation 9.

The Stephenson Equation 6 for a wind fetch of 518 km yields a wave height given by $H_{\max}$ = 0·336 × $(518)^{0{\cdot}5}$ = 7·6 m as opposed to 4·0 m quoted in Table 2. It is to be noted that the Stephenson empirical formula, however, refers to maximum wave height, whereas Table 2 quotes average height.

The Bretschneider Equations 7, 8 and 9 for a wind fetch of 518 km on a wind speed of 56 km/h (30 knots) for a duration of 23 h gives a wave height calculated at

$$H_s = 0{\cdot}0169 \times \left(30^2 \times 518/1{\cdot}858\right)^{0{\cdot}5} = 8{\cdot}5 \text{ m}$$

$$T_s = 0{\cdot}50 \times \left(30^2 \times 518/1{\cdot}858\right)^{0{\cdot}25} = 11{\cdot}20 \text{ s}$$

in comparison with the average period of 8·6 s quoted in Table 2.

$$F_{\min}/t_{\min} = 1{\cdot}14 \times 11{\cdot}20 = 12{\cdot}75$$

$$F_{\min} = (12{\cdot}75 \times 23) \times 1{\cdot}858 = 545 \text{ km} > 518 \text{ km}$$

$$H_s = 0{\cdot}0169 \times \left(30^2 \times 518/1{\cdot}858\right)^{0{\cdot}5} = 8{\cdot}5 \text{ m}$$

which again gives a greater value than the 4 m, noted from Table 2.

However, the significant wave height and significant wave period is the mean or average wave height of the highest third waves present in the wave train, which differs from the average height quoted in Table 2. It is further found that the significant height is nearly equal to the height reported from visual observations. The significant wave period represents a period around which is concentrated the maximum wave energy. Wave spectrums according to Pierson and Moskowitz (1964) and then followed by Jonswap (Hasselmann *et al*., 1973) also allow calculations of fetch.

Malta's climate is defined as well behaved with infrequent winds (e.g. hurricanes) not occurring. The most common wind in all seasons for Malta is the cool north-westerly (Maestrale) which blows on an average of 19% of the days in a year. Next in frequency are winds blowing from the NNW and W

Wind conditions			Wave size		
Wind speed in one direction	Fetch: km	Wind duration: h	Average height: m	Average wavelength: m	Average period: s
19 km/h (5·25 m/s)	19	2	0·27	8·5	3·0
37 km/h (10·25 m/s)	139	10	1·50	33·8	5·7
56 km/h (15·5 m/s)	518	23	4·10	76·5	8·6
74 km/h (20·5 m/s)	1313	42	8·50	136·0	11·4
92 km/h (25·5 m/s)	2627	69	14·80	212·2	14·3

Data source: Garrison (2002)

Table 2. Conditions necessary for a fully developed sea at given wind speeds and the parameters of the resulting waves

(Punent). All other winds are nearly equally represented and none show any dominance. However, the Maltese islands are definitely windy with only 7·7% of the days, on average, being calm with a wind speed of 0·5 m/s. Most other days have a wind speed between 0·5 and 11 m/s (1 and 21 knots). The prevailing winds are from directions 270 through to 300°, with minor secondary peaks from 90 and 180° as noted in Figure 4. Days with gusts of wind greater than 18 m/s (35 knots), which are termed gale force winds, occur throughout the year with a maximum frequency in December and a minimum in the months of June to September. Gales of force 8, with wind speeds varying from 23 to 30 m/s (45 to 58 knots) are much rarer and only occur on an average of 0·1 days during the months of January, February and October. In other words, only one day of January, February and October in a period of 10 years has force 8 winds. The strongest gale recorded was in December 1988 at 34 m/s (66 knots) (Chetcuti *et al.*, 1992).

A gentle/moderate breeze is given by a wind speed of 5 m/s, a fresh/strong breeze at 10 m/s, with a strong gale causing slight structural damage at 20 m/s. At 25 m/s tress are uprooted, and at wind speeds greater than 32·5 m/s the countryside is devastated, but these only occur in tropical countries. A more detailed outline of the Beaufort wind scale with anticipated waves is given in Table 3.

The Maltese Archipelago is subjected to 3 m wave heights from the Grigal winds (NE), with an 647 km fetch (Figure 1) facing from the Greek Adriatic Coast, whereas from the Maestrale (W–E) with a 587 km fetch (Figure 1) wave heights up to 5·2 m have been noted over a period spanning from 1958 to 2001 (according to the EU's WERMED project of 2004–2006; http://www.capemalta.net/maria/pages/climatologies.html). The above maximum wave heights recorded from varying directions relate to a reduced wind speed from the Grigal as opposed to the Maestrale.

For a Grigal NE maximum wind speed of 11 to 17 knots (Figure 4), fetch of 647 km with a 3·0 m wave height (according to WERMED), this is to be compared with Table 2 data for wind fetch at 518 km at 15·5 m/s wind speed (force 6) giving an average wave height of 4·1 m. For a Maestrale N-W maximum wind speed greater than 22 knots (Figure 4), fetch of 587 km with a 5·2 m wave height (according to WERMED), this again is to be compared with the Table 2 data value of 4·1 m as just noted. On the other hand the NWW fetch is given at 1286 km (Figure 1), maximum wind speed of 17 to 22 knots (Figure 4), whereas for the east direction the fetch is given at 1898 km, with maximum wind speed of 11 to 17 knots (Figure 4). The Table 2 wind fetch of 1312 km at 20·5 m/s wind speed (force 8) outlines an average wave height of 8·5 m – a wave height that has not been recorded around the Maltese islands.

4. Sea wave pressures on vertical faces

The power of the wind-driven waves has been established from actual measurements, together with the theory used depending on whether the walls are subjected to non-breaking (or pulsating), impulsive breaking (impact) or broken wave impact.

Forman (1909: p. 291) gives an interesting insight into the pressures created.

> Perhaps the most interesting experiments on the subject of the force of waves are those, which were carried out by Mr. Thomas Stevenson with the marine dynamometer designed by himself. The greatest force recorded during his experiments was one of 3·5 tons per square foot [335 kN/m^2], this pressure being obtained at Dunbar during an exceptionally severe storm about 1850. From the whole of his experiments it is probable that the average maximum force of waves does not much exceed 6,000 lbs per square foot

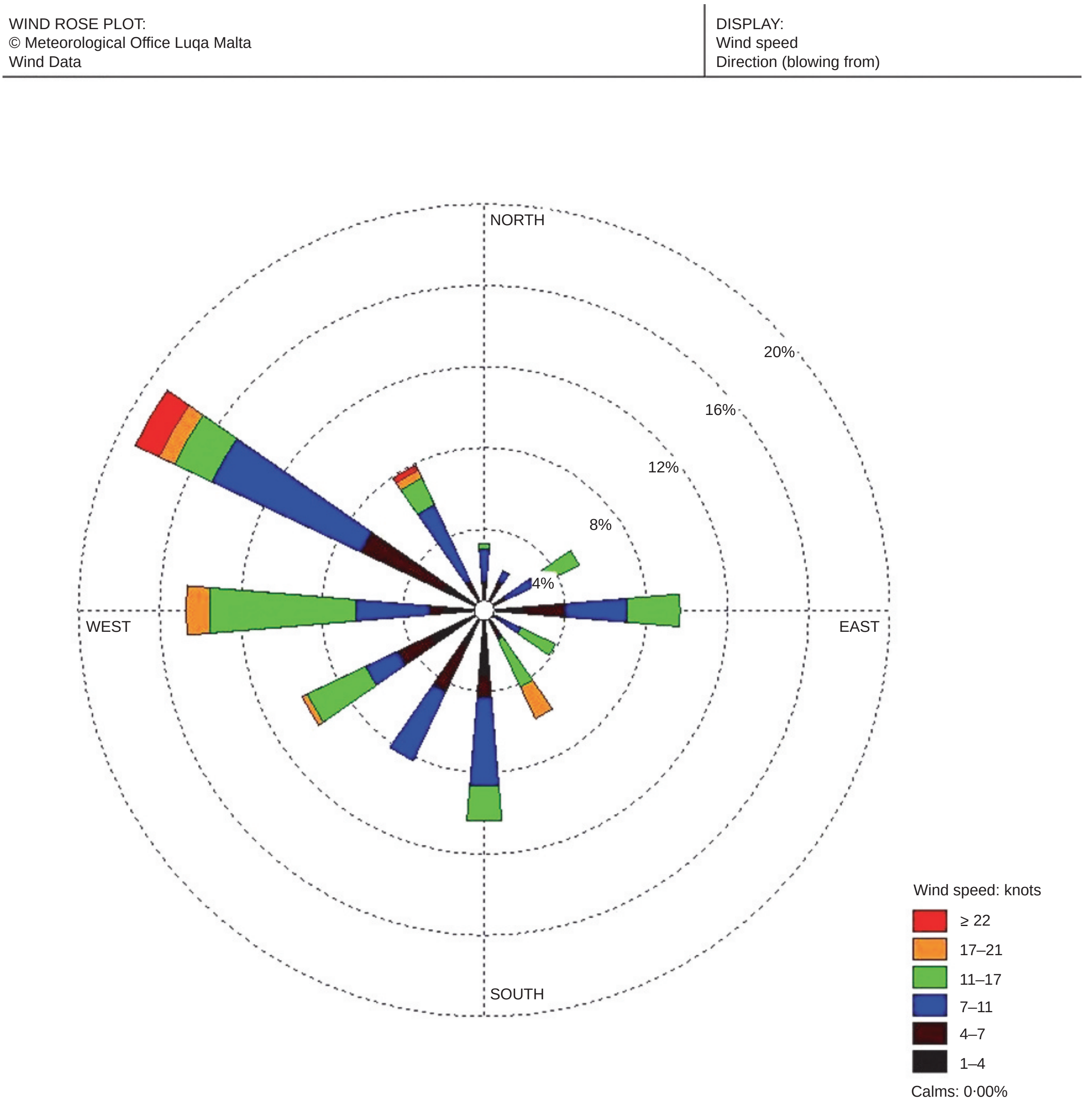

Figure 4. Wind rose for Malta: showing wind speed and direction during December 2008. Source Met Office January Newsletter 2009 (http://www.maltairport.com)

[287 kN/m^2], for any surface greater than 1 square foot in area, which in itself, however, is a very large pressure.

One thing that appears to be evident from Mr. Stevenson's experiments is that the larger the area of the exposed face of the dynamometer the less is the pressure recorded, which points to the fact that very high pressures, possibly even exceeding the record of 3·5 tons, may occur on small areas, even while the surrounding pressure is much less. Such concentrated pressures are a great source of danger to sea-walls, and have frequently led to failure.

Force	Description term		Wind speeds		Wave height: m	
	Wind	Wave	Knots	m/s	Probable	Maximum
0	Calm	–	< 1	0–0·2	–	–
1	Light air	Ripples	1–3	0·3–1·5	0·1	0·1
2	Light breeze	Small wavelets	4–6	1·6–3·3	0·2	0·3
3	Gentle breeze	Large wavelets	7–10	3·4–5·4	0·6	1·0
4	Moderate breeze	Small waves	11–16	5·5–7·9	1·0	1·5
5	Fresh breeze	Moderate waves	17–21	8·0–10·7	2·0	2·5
6	Strong breeze	Large waves	22–27	10·8–13·8	3·0	4·0
7	Near gale	Large waves	28–33	13·9–17·1	4·0	5·5
8	Gale	Moderately high waves	34–40	17·2–20·7	6·0	7·5
9	Strong gale	High waves	41–47	20·8–24·4	7·0	10·0
10	Storm	Very high waves	48–55	24·5–28·4	9·0	12·5
11	Violent storm	Exceptionally high waves	56–63	28·5–32·6	11·5	16·0
12	Hurricane	Exceptionally high waves	64–71	32·7–36·9	14·0	> 16

Data source: http://www.peardrop.co.uk/beaufort.htm.

Table 3. Beaufort scale and probable wave height

Gibson (1912: p. 276) refers to

> ... the maximum pressure produced by sudden impact is the same as is exerted by a steady jet, and is given, within about 1 per cent., by H or $v^2/2g$ metres of water, where H is the effective head producing flow measured above the point of impact.
>
> ... [Stevenson′s] values correspond with heads of 122 [37 m] and 105 feet [32 m] and with velocities of 89 [27 m/s] and 82·3 feet per second [25 m/s]. The mass of water being diverted by the face of the breakwater would then be projected upwards to a height approximately the same as that corresponding with these heads. As the result of observation, it is known that on the breaking of a wave during a storm, masses of water are, on occasion, hurled to heights in the neighbourhood of 150 feet [45 m] ...

The main methods used to estimate pulsating wave forces on upright breakwaters, include the work of Hiroi in 1919, Ito in 1971 and Goda in 1985. Sanflou in 1928, however, deals with walls in deep water, not subjected to impact forces. Minikin's method in the early 1950s, used for breaking waves was found to be too conservative, and has been overtaken by Goda's method used for both breaking and non-breaking waves. See Goda (2000) for a discussion of the methods mentioned in this paragraph.

Hiroi came up with the equation for uniform pressure P of the vertical wall given by

10. $$P = 1{\cdot}5\rho_{\mathrm{w}}gH$$

where ρ_{w} is the density of the sea given as 1025 kg/m^3; g is the gravitation of the earth (9·81 m/s^2); and H is the wave height (m). $\rho_{\mathrm{w}}g$ is given directly as 10·05 kN/m^3.

This wave pressure extends 1·25H above the mean sea water level or the crest of the breakwater if this is lower. Hiroi further gave an indication for the wave height to be taken as 0·9 times the depth of the water, if this is unknown. This should be the design wave, which as Goda notes for breakwater design works out at 1·8 times the expected wave (Goda, 1995).

With the Mediterranean significant wave height taken at 6·0 m, the breakwater design wave is taken at: 6·0 m × 1·8 = 10·8 m.

Hiroi's method (Equation 10) gives a wave pressure of

$$P = 1{\cdot}5 \times 10{\cdot}05\ \mathrm{kN/m^3} \times 10{\cdot}8\ \mathrm{m} = 163\ \mathrm{kN/m^2}$$

This wave pressure is just under half the localised value as measured by Stevenson at 335 kN/m^2. Typical impact pressure (Alderney, P = 400 kN/m^2, t = 15–30 ms) (Bredmose *et al.*, 2003; Bullock and Obhrai, 2004).

These wave pressures are considerable, noting that gas explosion loading is designed for 35 kN/m^2. This peak value below the still water line decays rapidly with depth, although not being the case of the Hiroi method. According to experiments undertaken by Luiggi on the Genova breakwater, this pressure reduces by half over a 3·0 m depth, halving again over the next 3·0 m depth. Thus, the Hiroi wave pressure thus calculated above averages out this decay in wave pressure over the wall's depth. A Construction Industry Research and Information Association (Ciria) document (Thomas and Hall, 1992) notes that the average wave pressure on sea walls varies from 150 kN/m^2 down to 50 kN/m^2, with the lower pressures adopted where the wall is very high.

The actual horizontal force on a 7 m high breakwater is calculated at

$$F_{\mathrm{h}} = 7\ \mathrm{m} \times 163\ \mathrm{kN/m^2} = 1141\ \mathrm{kN/m^2}$$

The hydrostatic force F_{w} equates to $0{\cdot}5\rho_{\mathrm{w}}gH^2$

$$F_{\mathrm{w}} = \left[10{\cdot}05\ \mathrm{kN/m^3}\ \times (7\ \mathrm{m}\ \times 7\ \mathrm{m}\ )\right]/2 = 246\ \mathrm{kN/m}$$

Thus the actual wave breaking force F_{t} on the breakwater equates to 1141/246=4·65 times the hydrostatic force, with the average hydrostatic pressure $P_{\mathrm{w}} = 0{\cdot}5\rho_{\mathrm{w}}gH$ for a 7 m high wall averaging out to

$$P_{\mathrm{w}} = \left(7\ \mathrm{m}\ \times\ 10{\cdot}05\ \mathrm{kN/m^3}\right)/2 = 35\ \mathrm{kN/m^2}$$

This is compared with the Hiroi uniform pressure given above as 163 kN/m^2.

Reference is made to a *Coastal Engineering Technical Note* (USACE, 1988) introducing the Goda method to replace the Minikin method. The now superseded *Shore Protection Manual* (USACE, 1984) had cautioned its users on the high forces that were obtained by the Minikin method, although it is now not mentioned in the latest edition (USACE, 2002). An inconsistency arises as in the *Coastal Engineering Manual* (USACE, 2002), this method is considered unreliable as it leads to high pressures for short waves, but is then recommended in cases in which severe breaking wave pressure arises. Another advantage of the Minikin method is that it may be undertaken by a hand calculation. A less conservative method recommended by Goda (1974) is an alternative procedure for breaking wave force determination. The rationale of using the Goda method for design analysis is that the duration of the impulsive breaking force is relatively brief, of in the order of one-tenth or one-hundredth of a second, and the effect of this force on the stability of massive concrete wall structures, particularly those with rubble mound bases, may be rather insignificant.

The following technical note gives the impulsive wave forces on a 4·3 m high wall with a 2·5 m water height and wave periods of 6 and 10 s, for both the Goda and the Minikin methods, summarised in Table 4.

For a 4·3 m high wall the Hiroi method gives a force F_{h} of 278 kN/m, which equates to three times the hydrostatic force developed over this 4·3 m high wall. The bold figures clearly indicate the conservative figures given by both the Hiroi and Minikin method in comparison with the Goda method, with forces equating to 1·2 times the hydrostatic pressure developed.

For vertical-walled structures where waves are depth limited, wave breaking may significantly reduce waves under the largest storms before they reach the structure. Wave forces under broken waves are therefore much lower than impact loads and may be indeed lower than pulsating loads. A method to estimate an average wave pressure from broken wave loads has been developed by Blackmore and Hewson (1984). This is given by the equation

$$P_{\max} = \lambda\rho_{\mathrm{w}}v_{\mathrm{c}}^2T \qquad (11)$$

where λ is an aeration coefficient taken as 0·3 for a sand bed and 0·6 for a rock bed; ρ_{w} is the water density; v_{c} is the velocity of the breaker at the wall = $(gD)^{0{\cdot}5}$; and T is the wave period.

The recorded impact pressure by this method is 48·6 kN/m^2 (Munireddy and Neelamini, 2004).

	Goda method		Minikin method	
Wave period: s	6·0	10·0	6	10
Pressure, P_1: kN/m^2	26·6	36·4	336	176
Force, F_{h}: kN/m	99·6	142·0	309	194
Bending moment, M: kN-m/m	204·0	289·0	772	485

Data source: USACE (1988).

Table 4. Comparison of wave forces on a 4·3 m high wall as calculated by the Goda and Minikin methods

5. Tsunami pressures on vertical faces

As noted in Section 2, tsunami waves are defined as shallow such that Equation 1 is applicable to determine their velocity of travel.

Table 5 has been calculated from the shallow water approximation, although with the rapid accelerations and decelerations associated with turbulent flow in fast-moving tsunami bore and surges, Keulegan (1950) had updated the shallow water relationship to

12. $$V=(gD)^{0\cdot 5}$$

according to natural environment research as part of Coventry University and University College London's Tsunami Risks Project (http://www.nerc-bas.ac.uk/tsunami-risks/index.html). A non-breaking wave, unlike a breaking wave due to limited drag forces, develops a larger inundation distance. The energy of a wave becomes less concentrated as the wave spreads. Thus, a tsunami has more energy when it strikes a shoreline that is relatively close to its point of origin, than it does when it reaches a distant coast. From the normal shoreline bathymetry features outlined previously, as the tsunami approaches land, the wave slows down, the height of the wave increases and its wavelength decreases. Deep water close to the shore, on the other hand, hampers the build-up of a very high wave. An enormous wall of water builds-up and then inundates the land in a tide-like flood. The surge momentum may increase the wave height at shoreline to give a run-up height being two to five times when particle velocity within the wave exceeds the wave velocity for a breaking wave, while a non-breaking wave does not amplify the run-up height. This build-up may be higher than 30 m for tsunami waves generated near the earthquake's epicentre or 15 m for tsunamis of distant origin, but even a tsunami 3 to 6 m high may be very destructive.

Depth: m	Velocity: km/h	Wave length: km
7000	943	282
4000	713	213
2000	504	151
200	159	48
50	79	23
10	36	10·6

Data source: IOC (2002).

Table 5. Velocity and wavelength of tsunami wave for given ocean depth

Tsunamis, although with rarely breaking waves, are very destructive because of the much higher breaking water velocities, with onshore velocities for the 2004 Indian Ocean disaster ranging from 18 to 47 km/h (5 to 13 m/s), while noting that velocities of 10 km/h (2·5 m/s) for a river is considered to be fast flowing. Observed flow velocities in historical tsunamis have been inferred to be of the order of 10 to 30 m/s (Blong *et al.*, 2005). Even considering a velocity < 5 m/s and wave height < 5 m, forces exceed 50 kN/m^2 with windows and masonry panels expected to fail at 10 to 20% of this level (Pomonis *et al.*, 2005).

The total horizontal force is given by the addition of the hydrostatic, hydrodynamic impulsive and inertial force acting on the impinging structure. The buoyancy forces, hydrodynamic lift, and weight of water inside the structure (Hinwood, 2005) give the vertical force. This is a form of the Morrison equation, which consists of two parts: a drag force F_D and an inertia force F_I given by

13. $$F_D=0\cdot 5\rho_w C_d B U^2$$

14. $$F_I=\rho_w C_m U \mathrm{d}U/\mathrm{d}t$$

In the above equations, ρ_w is the density of seawater, C_d is the drag coefficient, B is the frontal wall area, U is the water particle velocity, C_m is the inertia coefficient, and $\mathrm{d}U/\mathrm{d}t$ is the total water particle acceleration.

The Federal Emergency Management Agency (FEMA, 2003) recommends a drag coefficient C_d of 1·25 for width to inundation depth ratios of 1 to 12 for water taken normal to the house wall; hydrodynamic loading per unit length of the wall is five times that of the hydrostatic pressure. The impact coefficient C_m is taken to be between 1·7 and 3, and for this range may be 12 times that of the hydrostatic force. Thus the overall loading may be as much as 18 times the hydrostatic force. A Japanese design method (Okada *et al.*, 2004) for tsunami wave loading considers both the static and the dynamic loads together. The force per unit length of the wall is taken as an equivalent hydrostatic load with three times the inundation depth, H, for a tsunami wave for no break-up. This leads to a resultant force equal to nine times the hydrostatic force of inundation depth H. In the case of a wave break-up, an additional triangular pressure distribution to a height of $0\cdot 8H$ with base pressure of $2\cdot 4\rho_w gH$, where ρ_w is the seawater density, is superimposed.

The total tsunami force F_t for a breaking wave works out at

$$0\cdot 5\rho_w g(3H)^2+0\cdot 5(2\cdot 4\rho_w g)0\cdot 8H=5\cdot 46\rho_w gH^2$$

This leads to an equivalent force of around 11 times the hydrostatic force of inundation depth H, as the hydrostatic force on a wall of height H works out at $0{\cdot}5\rho_w gH^2$. If the height of the building is less than $3H$, then the pressure distribution is truncated at the height of the building.

The above thus suggests that the wave loading may be as high as 18 times the hydrostatic force with the lowest quoted at nine times. Model testing undertaken of a new tsunami-resistant house design and a typical Sri Lankan coastal house in a wave tank suggests that the maximum wave loading on house walls, at wave impact was 10 to 12 times the hydrostatic force (Thusyanathan and Madabhushi, 2008).

In the more exposed parts of the Mediterranean, a 1·5 m high run-up has a return period of 100 years, with a 500-year return period for a 4·0 m high run-up and a 1000-year return period for a 7·0 m run-up (Tiedemann, 1992). Most Mediterranean tsunami sources lie along mainland and island coastal regions, with tsunamis reaching local coasts soon after they have been generated, giving little time for warning, varying from 1 to 30 min. Table 6 outlines the principal tsunamigenic zones of the Mediterranean.

The tsunami intensity I is given by Ambraseys (1962) where

15. $I = \log_2 H^{0{\cdot}5}$

Equation 15 signifies that for I with an intensity III tsunami, wave run-up is calculated at 2 m. Squaring up then occurs for each successive intensity scale. This signifies that at intenisty VI, wave run-up is calculated at 64 m.

Site-specific evaluations to tsunami hazard are defined as those < 3–5 m above sea level or 7–10 m in the case of the most hazardous regions. Once the hazard of the wave run-up has been defined, the potential inundation zone (IDZ) is defined as the area between the coastline and the contour of the highest recorded tsunami.

The tsunami risks for the Maltese Archipelago have been identified by Camilleri (2006) with return periods for a 4 and 7 m high tsunami wave identified at 600 and 1500 years, respectively. The tsunami modelling undertaken has established that the greatest tsunami damage with 5·00 m height run-off is expected from the Aegean Sea within a 90 min warning, whereas from eastern Sicily only a 0·5 m high run-off is expected within a 50 min warning period (Ruangrassamee, 2008).

Thus, for a 4·3 m high tsunami Malta breaking wave, the force impact at 11 times the hydrostatic force is calculated as

$$\begin{aligned} &11\left(0{\cdot}5\rho g H^2\right) = \\ &11 \times \left\{\left[10{\cdot}05\ \text{kN/m}^3 \times (4{\cdot}3\ \text{m} \times 4{\cdot}3\ \text{m})\right]/2\right\} \\ &= 1022\ \text{kN/m} \end{aligned}$$

Coastal region	Average recurrence: years	Intensity, I Average	Maximal	Year of last tsunami	Probability of next tsunami
North Aegean	22	2·4	III	1978	Low
Eastern Greece	26	3·1	IV	1956	High
South Turkey	18	2·6	III	1961	High
Aegean Sea	9	3·7	X	1968	High
Hellenic island arc	21	3·5	VI	1948	High
Cyprus	17?	3·5	V?	1979	Low
Eastern Mediterranean	106	3·2	V	1870	Medium
Western Greece	14	–	VI	1953	High
Corinthian Gulf	20	–	V	1981	Low
Albania	31	3·2	IV	1920	High
Yugoslavia	20	3·3	V	1979	Low
Venetian Gulf	180?	3·0	VI	1511	–
Eastern Italy	52	3·2	V	1889	High
Calabria/Sicily	12	3·8	VI	1954	High
Western Italy	46	3·5	V	1870	High
Ligurian Sea	17	2·8	IV	1914	High
Spain	100	3·0	III–IV	1860	High

Table 6. Characteristics of the principal Mediterranean tsunamigenic zones: data from Soloviev (1990)

	Impact force	% of tsunami impact
Tsunami	1022 kN/m	100
Hiroi	278 kN/m	27
Minikin	309 kN/m/194 kN/m	25
Goda	100 kN/m/142 kN/m	12

Table 7. Comparison of wind-driven and tsunami waves on a 4·3 m high wall

The average tsunami wave pressure works out at 1022/4·3= 238 kN/m^2.

Similarly for a 7 m high tsunami wave, this wave pressure works out at 387 kN/m^2.

From results established in the present study, this tsunami force is compared with similar 4·3 m high sea wind-driven waves as noted in Table 7.

The above tsunami wave pressures generated as calculated, which relate to solid wall faces, exclude the effect of impacting debris. Tests undertaken in Thailand (Lukkunaprasit *et al.*, 2009) ascertained the tsunami wave pressures generated with wall openings of 25 and 50%. Reductions were noted in the 15 to 25% and 30 to 40% ranges, respectively. The tsunami force generated was approximately four times higher than the force generated for the wind-driven waves as evaluated for the Hiroi and Minikin methods, whereas they were eight times higher than the force generated by the Goda method.

Tsunamis, although with rarely breaking waves, have been noted above as fast flowing and on reaching shallower coastal waters slow down and increase in height as the wave encounters less and less room, with the resulting piling of water into an enormous wall of destruction, unlike a wind-driven wave and then inundates the land in a tide-like flood. This explains the high tsunami impact force as noted in Table 7.

Unlike the tsunami wave, in the case of wind-driven waves this does not consist of a wall of water, but the wave will have entrapped pockets of air. This, on being compressed, causes an explosion to occur with the water shooting into the air in an aerated condition, with the peak shock pressure occurring only in the locality of the air cushion, and the pressures at the bottom of the wall tending to be only hydrostatic (Minikin, 1963). The wave theory used depends on whether the walls are subjected to non-breaking (or pulsating), impulsive breaking (impact) or broken wave action. Where wind-driven waves break at the vertical face of a structure, the resulting impact forces are substantially more intense than for the non-breaking wave loads. Minikin's method developed in the early 1950s estimated local wave impact pressures caused by a wave breaking directly onto a vertical breakwater or sea wall. On the other hand, a train of non-breaking waves approaching a vertical wall will be reflected to some degree and form a standing wave pattern, with Goda's method being the most widely used for vertical walls. Where waves are depth limited, broken waves form which, as noted earlier, may be calculated by the Blackmore and Hewson Equation 11. This gives a force lower than an impact load and indeed may be lower than pulsating loads (McConnell *et al.*, 2004). This explains why the Hiroi and Minikin impact forces in Table 6 are approximately double the Goda force.

6. Discussion and conclusions

Table 7 clearly demonstrates that the impact force for a tsunami wave is double the impact for a wind-driven wave of the same height, as noted by the Hiroi method. The Minikin method, on the other hand, demonstrates the tsunami's wave impact is four times greater, whereas the Goda's method gives this as eight times greater. The rationale of the Goda method quoted earlier on is that the infinitely short duration of the maximum impulsive breaking force is taken note of.

Stevenson had measured this maximum impulse wind-driven pressure at 335 kN/m^2 in the nineteenth century, whereas recent tests undertaken at Alderney give this wave pressure at 400 kN/m^2.

Model testing of tsunami waves gives average not maximum pressures and yields values of 238 kN/m^2 (4·3 m wall height) and 387 kN/m^2 (7·0 m wall height); these as based on 11 times the hydrostatic force for the specified wall height.

The various average wave pressures for the hydrostatic impulse forces developed are outlined in Table 8.

Table 8 demonstrates the maximum average wave pressure developed at 238 kN/m^2 for a tsunami wave, with the minimum of 28 kN/m^2 by the Goda method for wind-driven waves. For a 7·0 m high tsunami wave this pressure increases to 387 kN/m^2. As a comparison, blast explosions create pressures equivalent to 35 kN/m^2. The Ciria document quoted earlier then quotes design values for sea-wind-driven waves to be taken at 150 kN/m^2 down to 50 kN/m^2 for high walls. It should be noted that an average horizontal design wave pressure of 50 kN/m^2 is equivalent to a warehouse 12·5 m height vertical static stacking of metal goods.

It thus appears that while noting the short duration of impact waves, the design hydrostatic tsunami wave pressure may be reduced from the test results obtained at 11 to 12 times the hydrostatic force value. The Okada Japan Design Method also refers to hydrostatic forces developed of 9 to 11 times depending on whether breaking or non-breaking waves. Is it

	Tsunami	Hiroi (WD)	Minikin (WD)	Goda (WD)	Blackmore and Henson (WD)
Equivalent hydrostatic impact force	× 11	× 3	× 2·7	× 1·3	× 2·25
Average pressure: kN/m^2	238	65	58	28	48·6

WD, wind-driven.

Table 8. Hydrostatic pressures developed for a 4·3 m wall height with corresponding equivalent uniform pressures developed

also opportune to review this design method, to take account of the longer-term pressure duration? This was undertaken in the Goda wind-driven wave method.

Table 8 notes that the equivalent hydrostatic force to be taken for wind-driven waves varies from ×3 (Hiroi) down to ×1·3 (Goda), a downsizing of 2·25 times. Applying the same to tsunami forces, this downsizing reduces the equivalent hydrostatic force for a tsunami wave to ×5. For a 4·3 m high wall, this gives an average tsunami wave pressure of 108 kN/m^2, as opposed to the previous established pressure of 238 kN/m^2.

It is possible that further testing is required to establish the design impact force to be utilised by structural engineers in their structural design of materials as impacted by a tsunami wave. The effect of openings on the wall facing the impact wave should also be taken account of. Further, following the recent Japanese Fukushima Dai-ichi nuclear power plant fallout is the Okada Japan Design Method due to the overtopping tsunami waves to be updated?

There are 13 active volcanoes in the central Mediterranean area, with a chain density of 68 km. The general rate of activity is related to the chain density, being the average distance between alternate volcanoes in a particular region. Eruptions in central America, with an average chain density of 37 km, and Japan (42 km) are somewhat higher than in the central Mediterranean (68 km).

Mount Etna, situated 220 km due north of Malta, is the largest active volcano in Europe and erupts fairly regularly. Other volcanic areas include Pantelleria and Limosa, roughly in line with Malta. Further north are Ustica, the Aeolian Islands (340 km away), together with Vesuvius further still (570 km away). During AD 79 the volume of solid material ejected from Vesuvius during an explosive eruption was estimated at 4 km^3 (maximum recorded 1000 km^3). Vesuvius has a span of 5·27 years between each eruption, with a standard deviation of 4·8 years. The last eruption dates back to 1944, which could be an indication that a relatively violent event is probable now (Camilleri, 1999).

This Mediterranean vulcanism further explains the tsunami intensity incidence of the Mediterranean Sea. Historical records show the western Mediterranean to be less prone to damaging tsunamis than the east. The Maltese islands lie in the Sicily Channel, on the Pelagian Platform, a relatively stable plateau of the African foreland. The Pelagian Platform forms a shallow shelf separating the deep Ionian Basin from the western Mediterranean. Its sea-bed topography is characterised mainly by the NW trending Pantelleria rift, a system that features three grabens of Miocene–Pliocene age (Pantelleria Graben, Malta Graben and Linosa Graben) in which the water depth reaches a maximum of around 1700 m. The grabens are governed by a fault system that extends throughout the Sicily Channel from Southern Sicily to Tunisia and which has also been responsible for the major tectonic and geomorphological development of the Maltese islands. The grabens themselves are bounded by normal faults, trending mainly NW–SE, whereas a set of E–W trending features represent reactivated faults that now act as dextral transforms controlling the rift extension. The Malta Escarpment is a major geomorphological feature separating the Hyblean-Malta plateau from the deep Ionian Basin. It exhibits normal faulting with a minor sinstral strike slip component (Galea, 2007). Due to its stable surroundings, the Maltese islands are more prone to greater tsunami damage from the eastern Aegean Sea with a maximum wave height of 5 m. On the other hand, wind-driven sea damage for Malta is greater from the western Mediterranean with 5·2 m high sea waves developing due to the Maestrale NW winds, than from the eastern Mediterranean with 3·0 m high sea waves developing due to the Grigal NE winds. The wind rose diagram in Figure 4 explains the higher sea waves from the NW due to the higher wind speeds developing, as Figure 1 indicates the fetch distances for both these directions to be approximately equal. The wind rose diagram indicates a greater incidence of NW winds with maximum speeds exceeding 22 knots, whereas the lower incidence NE winds develop a maximum speed of 17 knots.

REFERENCES

Ambraseys NN (1962) Data for investigation of seismic sea waves in the eastern Mediterranean. *Bulletin of the Seismology Society of America* **52(4)**: 895–913.

Blackmore PA and Hewson P (1984) Experiments on full scale impact pressures. *Coastal Engineering* **8(4)**: 331–346.

Blong R, Weir B and Miliauskas B (2005) *GAPResponse 3: 26th December 2004 Indian Ocean Earthquake & Tsunami: The geophysical Event*. Benfield ReMetrics, Sydney, Australia.

Bredmose H, Peregrine H, Bullock G *et al*. (2003) Extreme wave impact pressures and the effect of aeration. *Proceedings of the 19th International Workshop on Water Waves and Floating Bodies, Cortona, Italy*. International Workshop on Water Waves and Floating Bodies, Oslo, Norway. See http://www.iwwwfb.org/Abstracts/iwwwfb19/iwwwfb19_04.pdf (accessed 26/01/2012).

Bretschneider C (1957) Revisions in wave forecasting: deep and shallow water. In *Proceedings of 6th Conference on Coastal Engineering, Gainesville, Florida*. Council on Wave Engineering, Engineering Foundation, New York, NY, USA, pp. 30–67.

Bullock G and Obhrai C (2004) *Wave Impact Loads at Large and Full Scale*. University of Plymouth, Plymouth, UK. See http://library.coastweb.info/602/1/Bullock.pdf (accessed 26/01/2012).

Camilleri DH (2006) Tsunami construction risks in the Mediterranean. *Disaster Prevention and Management* **15(1)**: 146–162.

Camilleri DH (1999) Vulnerability of buildings in Malta to earthquake, volcano and tsunami hazard. *The Structural Engineer* **77(22)**: 25–31.

Chesley SR and Ward SN (2006) A quantitative assessment of the human and economic hazard from impact-generated tsunami. *Journal of Natural Hazards* **38(3)**: 355–374.

Chetcuti D, Buhagiar A, Schembri PJ and Ventura F (1992) *The Climate of the Maltese Islands: a Review*. Malta University Press, Malta.

FEMA (Federal Emergency Management Agency) (2003) *Coastal Construction Manual (3 vols)*. FEMA, Washington, DC, USA, publication no. FEMA 55.

Forman JH (1909) Sea-walls and breakwaters. *Minutes of the Proceedings* **175(1909)**: 290–302, http://dx.doi.org/10.1680/imotp.1909.17411.

Galea P (2007) Seismic history of the Maltese islands and considerations on seismic risk. *Annals of Geophysics* **50(6)**: 725–740.

Garrison T (2002) *Oceanography: An Invitation to Marine Science,* 4th edn. Brooks/Cole, Belmont, CA, USA.

Gibson AH (1912) Wave-impact on engineering structures. *Minutes of the Proceedings* **187(1912)**: 274–291, http://dx.doi.org/10.1680/imotp.1912.16833.

Goda Y (1974) New wave pressure formula for composite breakwaters. In *Proceedings of the 14th International Conference on Coastal Engineering, Copenhagen, Denmark*. ASCE, New York, NY, USA, pp. 1702–1720.

Goda Y (1995) Japan's design practice in assessing wave forces on vertical breakwaters. In *Wave Forces on Inclined and Vertical Walls*. ASCE, New York, NY, USA, pp. 140–155.

Goda Y (2000) *Random Seas and Design of Maritime Structures,* 2nd edn. World Scientific, Singapore.

Hasselmann K, Barnett TP, Bouws E *et al*. (1973) Measurements of wind-wave growth and swell decay during the Joint North Sea Wave Project (JONSWAP). *Deutsche Hydrographische Zeitschrift* **Supplement 12**: A8.

Hinwood J (2005) Design for tsunamis – coastal engineering considerations. *Structural Engineering International* **15(3)**: 189–196.

OC (Intergovernmental Oceanographic Commission) (2008) *Tsunami – The Great Waves,* revised edn. UNESCO, Paris, France.

Keulegan GH (1950) Wave motion. In *Engineering Hydraulics*. Wiley, New York, NY, USA, chapter 11.

Lionello P and Sanna A (2005) Mediterranean wave climate variability and its links with NAO and Indian Monsoon. *Climate Dynamics* **25(6)**: 611–623.

Lionello P, Bhend J, Buzzi A *et al*. (2006) *Cyclones in the Mediterranean Region: Climatology and Effects on the Environment*. Elsevier, Amsterdam, the Netherlands.

Lukkunaprasit L, Ruangrassamee A and Thanasisathit N (2009) Tsunami loadings on buildings with openings. *Science of Tsunami Hazards* **28(5)**: 303–310.

McConnell K, Allsop W and Cruickshank I (2004) *Piers, Jetties and Related Structures Exposed to Waves – Guidelines for Hydraulic Loadings*. Thomas Telford, London, UK.

Minikin RR (1963) *Winds, Waves and Maritime Structures*. Griffin, London, UK.

Munireddy MG and Neelamini S (2004) Wave pressure reductions on vertical sea walls/cassions due to an offshore breakwater. *Indian Journal of Marine Science* **33(4)**: 329–337.

Okada T, Sagano T, Ishikawa T *et al*. (2004) *Structural Design Method of Building for Tsunami Resistance*. Building Technology Research Institute, Tokyo, Japan.

Pierson WJ and Moskowitz L (1964) A proposed spectral form for fully developed wind seas based on the similarity theory of S. A. Kitaigordskii. *Journal of Geophysical Research* **69(24)**: 5181–5190.

Pomonis A, Rossetto T, Wilkinson S *et al*. (2005) Concluding remarks. In *The Indian Ocean Tsunami 26th December 2004 – A Preliminary Report by EEFIT*. Institution of Structural Engineers, London, UK, pp. 42–43.

Ruangrassamee A (2008) *Tsunami Hazards in Malta and Development of Tsunami Database in the Mediterranean Sea*. IOI-Thailand, Bangkok, Thailand.

Soloviev SL (1990) Tsunamigenic zones in the Mediterranean Sea. *Natural Hazards* **3(2)**: 183–202.

Tiedemann H (1992) *Earthquake and Volcanic Eruptions: a*

Handbook on Risk Assessment. Swiss Re, Zurich, Switzerland.

Thomas RS and Hall B (1992) *Sea Wall Design*. CIRIA, London, UK.

Thusyanathan NI and Madabhushi SPG (2008) Tsunami wave loading on coastal houses: a model approach. *Proceedings of the Institution of Civil Engineers – Civil Engineering* **161(2)**: 77–86.

USACE (US Army Corps of Engineers) (1984) *Shore Protection Manual,* 4th edn. US Army Engineer Waterways Experiment Station, Washington, DC, USA.

USACE (1988) *Coastal Engineering Technical Note. Breaking Wave Forces on Vertical Walls*. US Army Engineers Waterway Experiment Station, Vicksburg, MI, USA, CETN III-38 3/88.

USACE (2002) *Coastal Engineering Manual*. US Army Corps of Engineers, Washington, DC, USA, Engineer Manual 1110-2-1100.